Materials Transactions, Vol. 50, No. 5 (2009) pp. 999 to 1003
Special Issue on Nano-Materials Science for Atomic Scale Modification

First Principles Lattice Dynamics Calculations of Ag^+ Doped KX (X = Cl, Br and I)

Hidenobu Murata[1,*], Tomoyuki Yamamoto[2] and Isao Tanaka[1,3]

[1]*Department of Materials Science and Engineering, Kyoto University, Kyoto 606-8501, Japan*
[2]*Faculty of Science and Engineering, Waseda University, Tokyo 169-8555, Japan*
[3]*Nanostructures Research Laboratory, Japan Fine Ceramics Centre, Nagoya 456-8587, Japan*

Phonon states of Ag doped potassium halides, KX:Ag^+ (X = Cl, Br and I), are computed by a first principles lattice dynamic method using 64-atoms supercells. Results are compared to experimental data in literature. Phonon density of states of host KCl and KI crystals satisfactorily agree to the experimental inelastic neutron scattering data. Experimental frequencies of the impurity-induced infra-red (IR) and Raman active modes in the low frequency region are reasonably well reproduced because the vibrations are localized within the first nearest neighbour anions of the Ag^+-ion. On the other hand, limitations of present calculations to reproduce the high frequency impurity-induced modes are pointed out. They are less localized to the Ag^+-ion. [doi:10.2320/matertrans.MC200815]

(Received November 28, 2008; Accepted February 3, 2009; Published March 25, 2009)

Keywords: *first principles calculations, phonon density of state, potassium halide, impurity doping, Raman spectroscopy, infrared spectroscopy*

1. Introduction

Most of first principles calculations in the past deal with crystals at the zero temperature. With the development of high performance computers as well as efficient numerical techniques, state-of-the-art first principles methods can calculate Hellmann-Feynman (H-F) force on atoms with reasonable accuracy. Once a set of forces associated with a set of small displacements on a crystal is obtained, phonon frequencies can be computed within the harmonic approximation. Many successful studies on the phonon calculations by the first principles methods have been reported.[1–5] However, most of them were carried out on perfect crystals, i.e., crystals without any defects. For calculations with defects, a large supercell is required to reduce artificial interactions among defects. Crystal symmetry becomes lower when defects are present. Phonon calculations of defective crystals are therefore much more demanding than those for perfect crystals. This is the reason why the number of first principles phonon calculations of defective crystals is still very limited.

In the present study, we aimed at calculation of phonon spectra in a model system with an impurity present in a simple crystal. We have chosen three potassium halides with rock-salt structures doped with Ag^+ ions. Experimental phonon dispersions of these host crystals were measured by neutron scattering method.[6–8] The impurity-induced vibration modes of KI:Ag^+ were extensively studied by Sievers and coworkers using Raman and IR spectroscopies.[9–13] In the present study, we examine the impurity vibrational states by first principles calculations. Results are compared with the experimental data in order to examine the accuracy and limitations of such calculations.

2. Computational Procedure

First principles calculations were made by a plane-wave basis projector augmented wave (PAW) method using VASP code.[14,15] Spin-polarized local density approximation (LDA)[16] was used for the exchange-correlation functional. After careful convergence tests, the plane-wave cut-off energy was set to be 350 eV and a $2 \times 2 \times 2$ of k-point mesh with Monkhorst-Pack scheme[17] was selected. Reference configurations for valence electrons for the PAW were $4d^{10}5s^1$, $3s^2 3p^6 4s^1$, $3s^2 3p^5$, $4s^2 4p^5$ and $5s^2 5p^5$ for Ag, K, Cl, Br and I, respectively.

Potassium halides, KX (X = Cl, Br and I), exhibit a rock-salt structure under ambient conditions. In the present study, we use a supercell consisting of 64 atoms which can be made by the $2 \times 2 \times 2$ expansion of a unit cell. As for the Ag^+ doped model, one of the K^+ ions in the supercell was replaced by an Ag^+ ion. Lattice constants and internal positions in the supercell were fully optimized until residual H-F force becomes smaller than 1×10^{-3} eV/Å.

Dynamical properties were computed by the frozen phonon method using fropho[18] code. The whole set of force constants were obtained from H-F forces generated by a set of nonequivalent atomic displacements in the supercell with the amplitude of 1 pm. Atomic mass averaged over naturally abundant isotopes was used for each atoms.

In an ionic crystal, atomic displacement induces a dipole. Dipole-dipole interaction remarkably affects the interatomic force constants and causes longitudinal optical/transverse optical (LO/TO) splitting at the wave vector of $\boldsymbol{k} \approx 0$, namely near the Γ point. In the present study, however, we do not take into account the influence of the dipole on the interatomic force constants. It does not change the conclusion of the present study.

3. Results and Discussion

The optimized cell parameters are summarized in Table 1. Our calculations underestimate experimental cell parameters of KX by less than 3%, which is within a typical range of errors by the LDA calculations. When one of K^+ ions in the supercell is substituted by an Ag^+ ion, the cell parameters

*Graduate Student, Kyoto University. Corresponding author, E-mail: hidenobu.murata@hw7.ecs.kyoto-u.ac.jp

Table 1 Calculated unit-cell parameters of KX and Ag^+ doped KX (X = Cl, Br and I). A half of the cell parameters of the $2 \times 2 \times 2$ supercell are shown for the Ag^+ doped models.

X	KX (nm)	Ag doped KX (nm)
Cl	0.6072	0.6047
Br	0.6363	0.6337
I	0.6810	0.6781

Table 2 Optimized ionic positions in the calculated $2 \times 2 \times 2$ supercells for $KX:Ag^+$ (X = Cl, Br and I).

		x	y	z
Ag		0	0	0
K(1)		0	0.248	0.248
K(2)		1/2	0	0
K(3)		1/2	0.250	0.250
K(4)		0	1/2	1/2
K(5)		1/2	1/2	1/2
X(1)	$KCl:Ag^+$	0.232	0	0
	$KBr:Ag^+$	0.231		
	$KI:Ag^+$	0.227		
X(2)		0.250	0.250	0.250
X(3)		0.249	1/2	0
X(4)		0.250	1/2	1/2

decrease by approximately 3 pm. This can be simply ascribed to the difference in ionic radius between K^+ (152 pm) and Ag^+ (129 pm).[19] Table 2 summarizes the atomic position of the doped crystals. Both cations and anions are labeled according to the distance from the Ag^+ ion. For example, X(1) denotes the first nearest neighbor (1-NN) anion of Ag^+. The internal coordinates denoted by either 0 or 1/2 correspond to atoms that are set immobile by symmetry constraints. Significant relaxation of atomic positions can be found only in the 1-NN shell of the Ag^+ ion.

The calculated total phonon DOS of the perfect crystals, i.e., KCl, KBr and KI, are shown in Figs. 1 to 3. Experimental phonon DOS by inelastic neutron scattering experiments for KCl and KI[6,8] are shown for comparison. Experimental DOS for KBr is not available to the authors' best knowledge. The present calculations are found to reproduce the experimental phonon DOS of KCl and KI except for the high frequency part in which LO/TO splitting contributes. In the calculated phonon DOS of KBr and KI, a gap in phonon DOS centered at 90–100 cm^{-1} can be clearly seen, while no such a gap can be seen in KCl. The gap in the host crystal can be ascribed to that between the acoustic and the optical branches. The gap is larger in KI since the difference in atomic masses between cation and anion is larger.

Phonon DOS of Ag^+ doped KCl, KBr and KI crystals by the present calculations are compared with those of the perfect crystals in Figs. 1–3. Roughly speaking, the calculated phonon DOS of Ag^+ doped models show similar profiles as those of host crystals. The phonon DOS is jagged and some new peaks appear in the doped models. Moreover in $KCl:Ag^+$, the distribution of the optical band located at

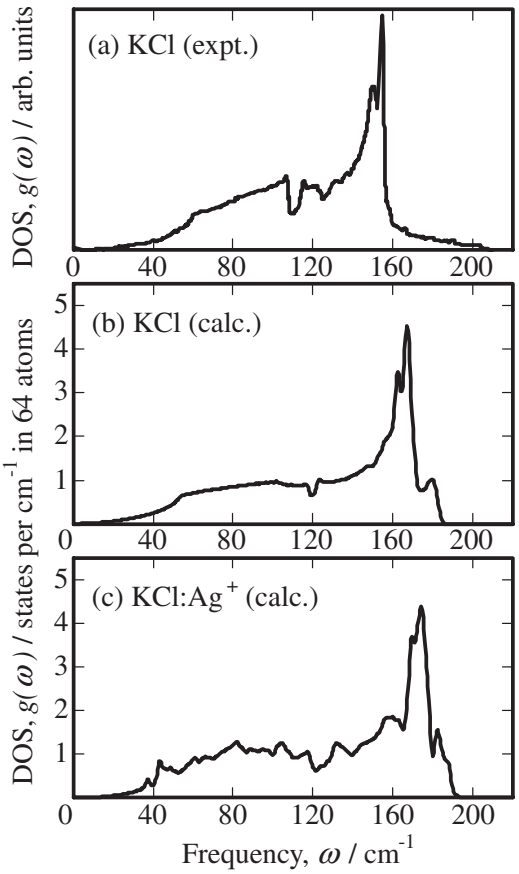

Fig. 1 (a) Experimental phonon density of states for KCl[6] and calculated total phonon density of states for (b) KCl and (c) $KCl:Ag^+$.

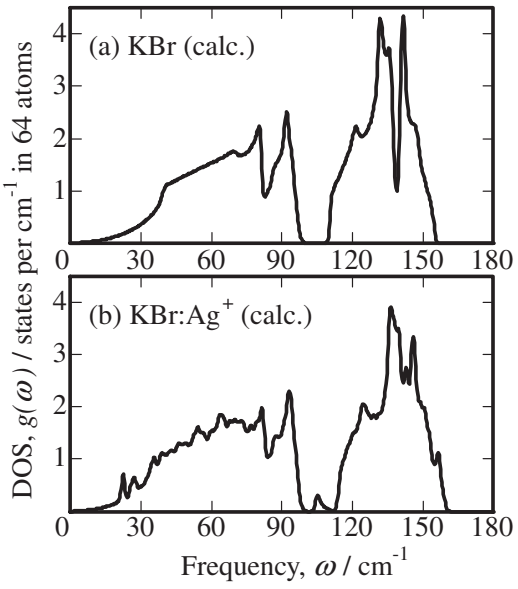

Fig. 2 (a) Calculated total phonon density of states for KBr and (b) $KBr:Ag^+$.

around 160 cm^{-1} is shifted to the higher energy side in the doped model.

The impurity-induced vibration modes of $KI:Ag^+$ were extensively studied by Sievers and coworkers using Raman and IR spectroscopies.[9–13] A few IR peaks in $KI:Ag^+$ were assigned as the Ag-impurity mode. Two of them, located

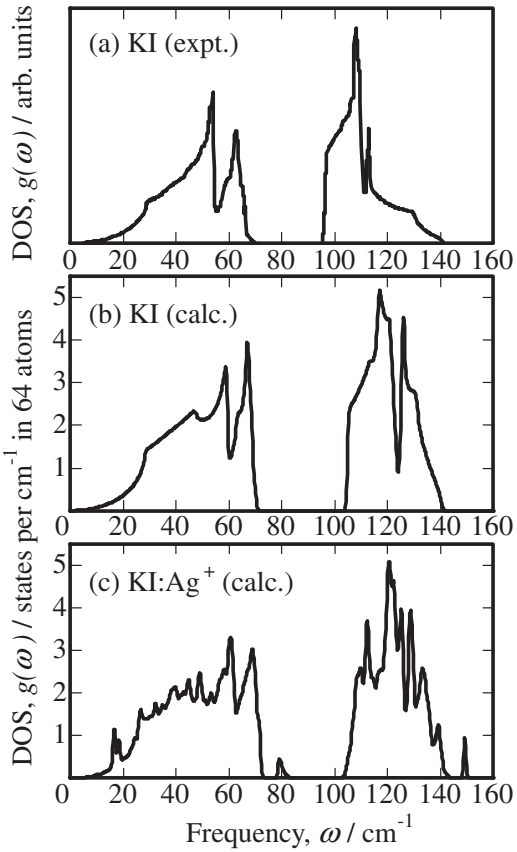

Fig. 3 (a) Experimental phonon density of states for KI[8] and calculated total phonon density of states for (b) KI and (c) $KI:Ag^+$.

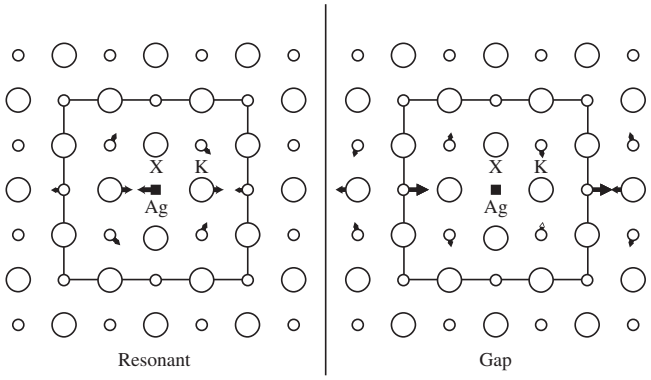

Fig. 4 Atomic displacements responsible to two IR active modes in $KI:Ag^+$ as reported in Ref. 13). A square corresponds to the 64 atoms supercell used in the present study.

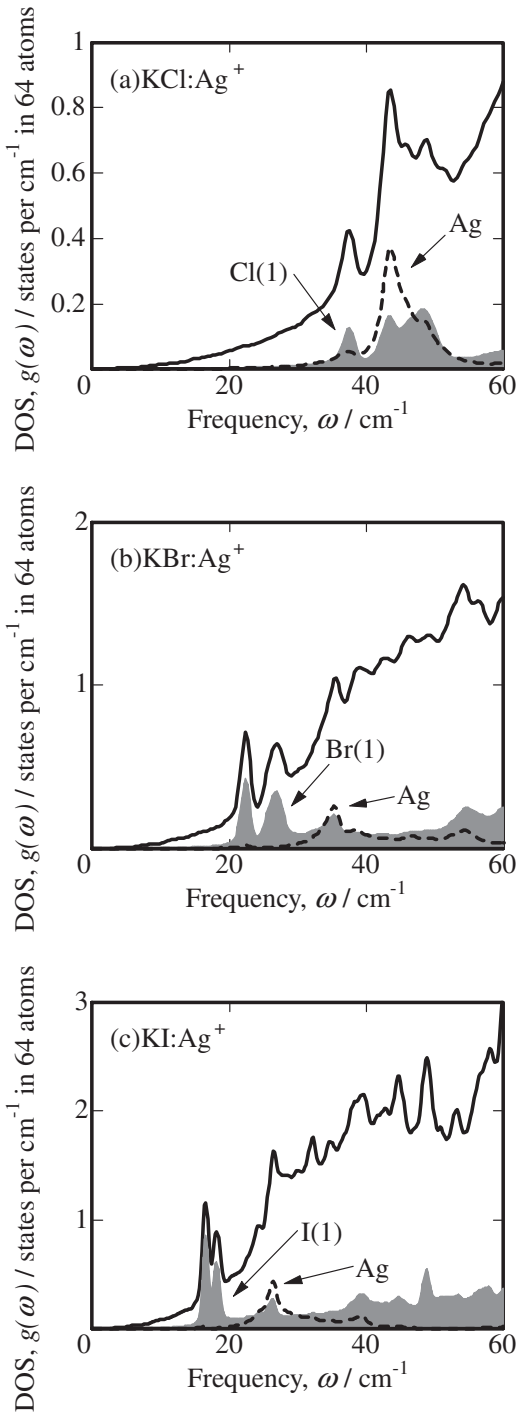

Fig. 5 Calculated phonon density of state of total (solid line), first nearest neighboring anions from doped Ag (X(1): dashed line) and Ag (gray area) for (a) $KCl:Ag^+$, (b) $KBr:Ag^+$ and (c) $KI:Ag^+$.

at 17.3 cm^{-1} and 86.2 cm^{-1}, are much stronger than the others. They are called a resonant mode and a gap mode, respectively. The displacement patterns corresponding to these modes were predicted on the basis of experimental observations and perturbed-shell-model calculations as shown in Fig. 4.[13] It is very interesting that the 86.2 cm^{-1} gap mode originates mainly from the atomic vibration of K(2) ions. The boundary of the 64-atoms supercell used in the present calculations is superposed on the model of Fig. 4. As can be found, the K(2) ions responsible for the 86.2 cm^{-1} peak are set immobile in the present calculations. We will hereafter discuss only the resonant mode.

The low frequency part of the calculated phonon DOS of three doped models are shown in Fig. 5(a)–5(c) together with the atom-resolved phonon DOS for the Ag^+ ion and X(1). A double peak can be seen in the calculated phonon DOS of $KI:Ag^+$ below 20 cm^{-1}. They originate from the vibration of I(1). Contribution of Ag^+-ion is very small. The impurity induced vibration states are localized to I(1). As a matter of fact, no such peaks can be found in the phonon DOS of the outer I-ions, i.e., I(2), I(3) and I(4), as will be shown in Fig. 6.

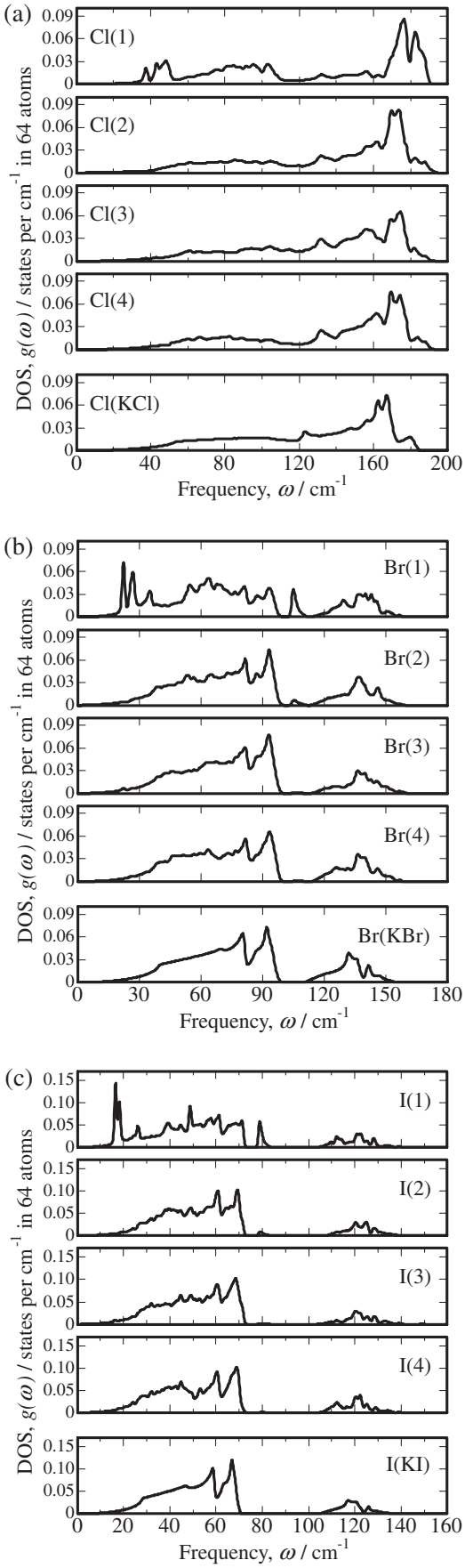

Fig. 6 Comparisons of projected phonon density of state of anions between pure potassium halides and Ag^+ doped (a) KCl, (b) KBr and (c) KI. Numbers in bracket are the types of anions, which are explained in Table 1.

Table 3 Comparison of impurity-induced Raman and IR frequencies in the acoustic band of host crystals between experiments and present calculations.

	Calc.(cm^{-1})		Expt.(cm^{-1})	
	IR (T_{1u})	Raman (E_g)	IR (T_{1u})	Raman (E_g)
KCl:Ag^+	39.5	51.3	38.8[11]	45[12]
KBr:Ag^+	27.8	28.1	33.5[9]	No data
KI:Ag^+	20.4	18.7	17.3[9]	16.35[10]

In addition to the experimental IR resonant mode at 17.3 cm^{-1}, an experimental Raman (E_g) mode was reported at 16.35 cm^{-1} in KI:Ag^+.[9,10] According to the present calculations, E_g and T_{1u} modes at the Γ point for KI:Ag^+ are found at 18.4 and 20.4 cm^{-1}, respectively. They should correspond to the Raman and IR modes found by experiments. Note that they do not coincide to the peak top frequencies of the phonon DOS because of the limitation due to the use of the small supercell in the present phonon calculations.

Similar impurity-induced peaks can be seen in the phonon DOS of KBr:Ag^+ and KCl:Ag^+. They also originate mainly from the vibration of Br(1) for KBr:Ag^+ and from the vibration of Cl(1) and Ag^+ for KCl:Ag^+. E_g and T_{1u} modes at the Γ point for all three systems are summarized in Table 3 together with the experimental IR and Raman frequencies in literature.[9–12] The present calculations show reasonable agreement to these experimental data in the low frequency region.

According to the present lattice dynamics calculations using the 64-atoms supercells, we found that impurity-induced IR and Raman active modes in the low frequency region can be reasonably well reproduced. At the same time, limitations due to the use of the small supercell can also be noted. Improper description of the gap modes in KI:Ag^+ and KBr:Ag^+ is a typical example. Figure 6(a)–6(c) show the calculated phonon DOS of three doped models with the atom-resolved phonon DOS for X (1), X (2), X (3) and X (4). They are compared to the calculated phonon DOS of X in undoped KX crystals. As can be seen, the effect of Ag-impurity is significant only on X(1) ion. The phonon DOS of the outer X-ions look similar to that of X in undoped KX. The present calculations using the 64-atoms supercells can therefore satisfactorily reproduce the low frequency resonant modes that are localized to the impurity. On the other hand, there are clear limitations to reproduce the high frequency gap modes. An impurity induced peak can be found in phonon DOS of KI:Ag^+ at around 80 cm^{-1}, which is close to the experimental gap mode IR frequency of 86.2 cm^{-1} by experiment.[10] However, as discussed at Fig. 4, the K(2) ions should be responsible for the 86.2 cm^{-1} peak, which are set immobile in the present calculations. Instead of K(2), I(1) and I(2) contribute to the 80 cm^{-1} peak in the computed result.

4. Summary

First principles lattice dynamics calculations are carried out to investigate the impurity induced phonon states in

$KX:Ag^+$ (X = Cl, Br and I) using the 64-atoms supercells. Results are compared to experimental data in literature. Phonon DOS of host KCl and KI crystals satisfactorily agree to the experimental data except for the high frequency part in which LO/TO splitting contributes. Frequencies of the impurity-induced IR and Raman active modes in the low frequency region are reasonably well reproduced by the present calculation. The atomic displacements responsible for these modes are localized at the X(1) ions for $KBr:Ag^+$ and $KI:Ag^+$. They are both Cl(1) and Ag^+ for $KCl:Ag^+$. On the other hand, limitations of present calculations to reproduce the high frequency impurity-induced modes are pointed out. They are less localized to the Ag^+-ion. This type of first principles lattice dynamics calculations can be useful for prediction of vibrational states of doped crystals, as long as limitations due to the use of a small supercell are taken into consideration.

Acknowledgement

This work was supported by Grant-in-Aid for Scientific Research on Priority Areas "Nano Materials Science for Atomic Scale Modification 474" from the Ministry of Education, Culture, Sports, Science and Technology (MEXT) of Japan.

REFERENCES

1) S. Wei, C. Li and M. Y. Chou: Phys. Rev. B **50** (1994) 14587–14590.
2) K. Parlinski, Z. Q. Li and Y. Kawazoe: Phys. Rev. Lett. **78** (1997) 4063–4066.
3) A. Kuwabara, T. Tohei, T. Yamamoto and I. Tanaka: Phys. Rev. B **71** (2005) 064301.
4) A. Kuwabara, K. Matsunaga and I. Tanaka: Phys. Rev. B **78** (2008) 064104.
5) T. Tohei, A. Kuwabara, F. Oba and I. Tanaka: Phys. Rev. B **73** (2006) 064304.
6) J. R. D. Copley, R. W. Macpherson and T. Timusk: Phys. Rev. **182** (1969) 965–972.
7) A. D. B. Wood, B. N. Brockhouse, R. A. Cowley and W. Cochran: Phys. Rev. **131** (1963) 1025–1029.
8) G. Dolling, R. A. Cowley, C. Schittenhelm and I. M. Thorson: Phys. Rev. **147** (1966) 577–582.
9) A. J. Sievers: Phys. Rev. Lett. **13** (1964) 310–312.
10) R. D. Kirby: Phys. Rev. B **4** (1971) 3557–3569.
11) A. J. Sievers: Elementary Excitations in Solids, ed by A. A. Maradudin and G. F. Nardelli: (New York: Plenum, 1969) p. 193.
12) W. Möller and R. Kaiser: Phys. Status Solidi **50b** (1972) 155–169.
13) A. Rosenberg, C. E. Mungan, A. J. Sievers, K. W. Sansudky and J. B. Page: Phys. Rev. B **46** (1992) 11507–11519.
14) G. Kresse and J. Furthmüller: Phys. Rev. B **54** (1996) 11169–11186.
15) G. Kresse and J. Furthmüller: Comput. Mater. Sci. **6** (1996) 15–50.
16) D. M. Ceperley and B. J. Alder: Phys. Rev. Lett. **45** (1980) 566–569.
17) H. J. Monkhorst and J. D. Pack: Phys. Rev. B **13** (1976) 5188–5192.
18) A. Togo, F. Oba and I. Tanaka: Phys. Rev. B **78** (2008) 134106.
19) R. D. Shannon: Acta Crystallogr. A **32** (1976) 751–767.